https://dx.doi.org/10.1016/j.jmatprotec.2019.116552

A novel magnetic field-assisted mass polishing of freeform surfaces

Chunjin Wang[a], Chi Fai Cheung[a,*], Lai Ting Ho[a], Kai Leung Yung[a] and Lingbao Kong[b]

[a]State Key Laboratory of Ultra-precision Machining Technology, Department of Industrial and Systems Engineering, The Hong Kong Polytechnic University, Hung Hom, Kowloon, Hong Kong SAR, China

[b]Shanghai Engineering Research Center of Ultra-Precision Optical Manufacturing, Fudan University, Shanghai, PR China

* Corresponding author. Tel.: +852 2766 7905.

E-mail address: benny.cheung@polyu.edu.hk (Benny C.F. Cheung).

Abstract

This paper presents a novel magnetic field-assisted mass polishing (MAMP) technology for high-efficiency finishing of a number of freeform components simultaneously. The MAMP makes use of a rotational magnetic field applied outside an annular chamber which drives the magnetic abrasives to impinge on and remove material from the workpiece mounted inside the chamber. The influence of the magnetic field on the material removal characteristics is analysed by the finite element method. The factors affecting surface generation were studied through polishing experiments. Experimental results show that MAMP is effective for polishing of a number of

freeform surfaces with nanometric surface finish.

Keywords: magnetic abrasive; magnetic field assisted; mass polishing; finishing; freeform surfaces; ultra-precision machining.

1. Introduction

Freeform surfaces have been widely used in various industrial applications, such as imaging, illumination, aerospace, biomedical engineering, green energy, etc. (Fang et al., 2013) And polishing is usually used as a finishing process to remove defects and tool marks from cutting and grinding processes (Fang et al., 2019). Nevertheless, the polishing process usually takes most of the time during the manufacturing process of precision freeform surfaces, which imposes a lot of challenges for meeting the increasing market demand. Hence, several kinds of mass finishing processes were developed to implement mass finishing of freeform surfaces, such as vibratory finishing, spindle finishing, centrifugal disc finishing, centrifugal barrel finishing and rotary barrel finishing as reported by Hashimoto and Johnson (2015). Hashimoto et al. (1996) conducted the vibratory finishing experiments on cylindrical specimens made of carburized steels, and the surface roughness (Ra) was improved from 0.28 μm to 0.06 μm. Davidson (2007) proposed a novel polishing process using dry abrasive and polishing media, which allows refined surface edge effects and avoids wet-waste discharge. Uhlmann and Eulitz (2018) found that the wear mechanism of conventional grinding tools can also be observed on the media in vibratory finishing. Li et al. (2018)

developed a new type of polyurethane media for the mass polishing of high performance parts with deep grooves and narrow slit, and 83.87% surface roughness improvement was obtained. However, those mass finishing methods can hardly achieve high surface form accuracy and nanometric surface finish.

The magnetic field-assisted polishing method has been used for polishing various kinds of surfaces for decades due to its high adaptability to the curved surfaces (Hashimoto et al., 2016), and various kinds of magnetic field assisted polishing method have been developed as reported by Komanduri et al. (1997) and Jain et al. (2009). Shinmura et al. (1990) conducted research on the finishing of roller surface based on magnetic field assisted finishing for the first time, and the initial surface roughness of 0.45 μm was largely reduced to 0.04 μm. Yamaguchi et al. (2000) further developed this technology and used a rotational magnetic field for the finishing of internal surfaces, even flexible capillaries that have inner diameter smaller than 1 mm (Yamaguchi et al., 2011). Yamaguchi et al. (2015) also proposed to use the hybrid loose and fixed abrasive tool for the capillary finishing, which solved the problem of the tool abrasive insertion. Chang et al. (2002) conducted magnetic field assisted polishing of roller surface, and the polished surface roughness was smaller than 0.1 μm. Except for the polishing of roller surfaces, Kordonski and Jacobs (1996) proposed the magnetorheological finishing (MRF) method for the superfinishing of optical freeform surfaces, which is capable of obtaining sub-nanometer surface roughness. And the material removal in MRF is highly deterministic and stable without tool wear. (Zhang et al., 2019) Jha and Jain (2004) innovatively developed the magnetorheological abrasive flow finishing

method, and the experimental results proved that it is an effective way for the finishing of the internal surface. Furuya et al. (2008) proposed a contact-free surface finishing method, which used the magnetic compound fluid to polish the metal structure surface. Singh et al. (2011) designed a ball end magnetorheological finishing tool, which is capable of finishing both ferromagnetic and nonmagnetic materials of 3D shapes. Yamaguchi and Graziano (2014) tried to improve the surface roughness of the cobalt chromium alloy bio-implants through utilizing the magnetic abrasive finishing method. Kumar and Jain (2015) also explored a rotating type magnetorheological abrasive flow finishing method for the polishing of femoral knee components. Guo et al. (2017) investigated the effect of different magnetic abrasives to the polished surface topography, and presented an innovative way for the polishing of double-layered tube structure surface based on magnetic abrasive polishing method which combining the rotation and vibration movement (Guo et al., 2019). Li et al. (2018) developed a semi-solid polishing media for magnetic field assisted finishing to improve the usage efficiency of the magnetic abrasive, and 96.67% surface roughness improvement was obtained on 6061 aluminum alloy tube. Nevertheless, most of the current applications of magnetic field-assisted polishing only polish one workpiece in one setup which makes the polishing process time-consuming and high-cost.

This paper presents a novel polishing method named magnetic field-assisted mass polishing (MAMP) which attempts the mass finishing of a number of freeform surfaces in one setup with nanometric surface finish. The polishing performance of this novel polishing technology has been demonstrated, and the effect of the key factors affecting

material removal characteristics have also discussed.

2. Methodology

2.1 Principle of magnetic field-assisted mass polishing (MAMP)

The schematic diagram of the MAMP system is presented in Fig. 1. In this method, an array of magnetic pole pairs is controlled to rotate along an annular chamber such that the magnetic abrasives inside the chamber generate magnetic brushes under the action of the magnetic field. The chamber is fixed and does not rotate during polishing while the magnetic brushes inside the chamber are driven by the rotating magnetic pole pairs. The abrasives inside the brush keep impinging the workpiece to remove material from the surface. At least two pairs of magnetic poles should be assembled in this system to maintain the balance of the rotating table while it is rotating, as shown in Fig. 1.

Six samples were polished simultaneously for the case in Fig.1. The magnetic brush is formed of bonded magnetic abrasives mixed with lubricant or loose (also named 'unbonded') magnetic abrasives mixed with carrier fluid. The bonded magnetic abrasives are fabricated by bonding the magnetic particles with the polishing abrasives, such as alumina, silicon carbide, diamond abrasive, etc. The loose magnetic abrasives are the magnetic particles mixing with the polishing abrasives in the base fluid. Movement of the magnetic force drives the polishing abrasives to impinge on the target surface and remove material by the abrasive force of the bonded or loose magnetic abrasives. The magnetic force F is given by Eq. (1) (Shinmura et al., 1990):

$$F_x = V\chi H\left(\partial H/\partial x\right), F_y = V\chi H\left(\partial H/\partial y\right) \quad (1)$$

where V signifies the volume of the magnetic particle, H signifies the magnetic field strength at the point P, χ is the susceptibility of the magnetic particle, $\partial H/\partial x$ and $\partial H/\partial y$ are the gradients of magnetic field strength in the x and y directions, respectively. The magnetic force is found to be proportional to the magnetic field strength and its gradient, magnetic particle susceptibility, and volume of magnetic particle.

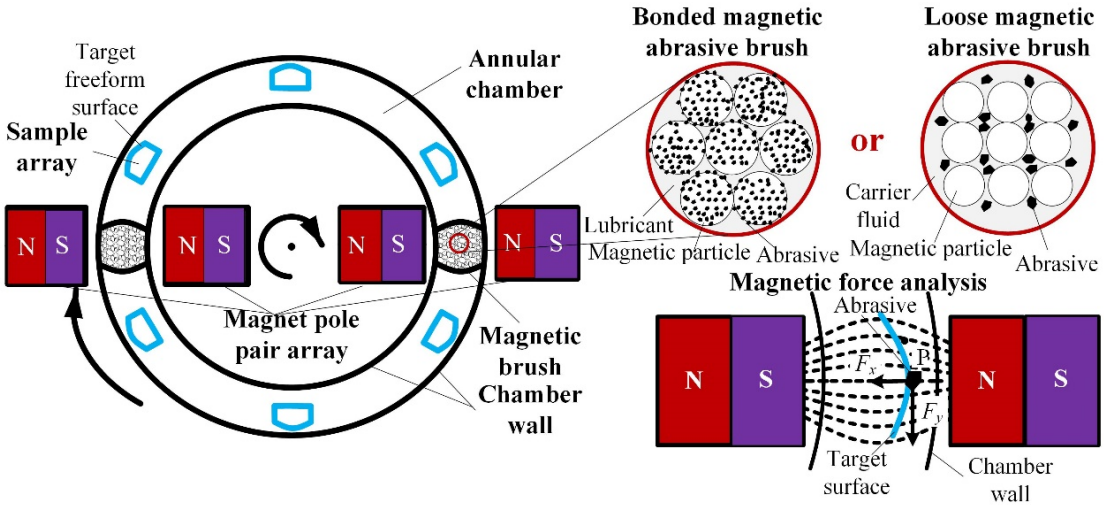

Fig. 1. Operation principle of magnetic field-assisted mass polishing

2.2 Finite element analysis of the magnetic field distribution

To gain further understanding of the working principle of this MAMP process, the magnetic field distribution under the polishing circumstances was modelled based on the finite element method (FEM), and implemented in the ANSYS software package. Fig. 2 shows the results of modelling and simulations of the magnetic flux density distribution. Half of the model was built to simplify the simulation model as shown in Fig. 2(b). Four N52 Neodymium permanent magnets were used in this FEM model,

whose size was 25.4 mm×25.4 mm × 50.8 mm. Its residual magnetic flux density was 1.45 tesla (T), and the coercive field force was 973000 amperes per metre (A/m). The material of the annular chamber was made of Polytetrafluoroethylene (PTFE) which is non-magnetic conductive material. A half model was used to simplify the calculation process. Fig. 2(c) show the simulated magnetic flux density B distribution in two sectional views. The relationship between B and H is expressed by Eq. (2):

$$B = \mu H = \mu_0 (1 + \chi) H \tag{2}$$

where μ_0 is the free space permeability. It is important to note that the magnetic flux density between the magnetic poles is much stronger than that for other zones inside the chamber, which explains the generation of the magnetic brush.

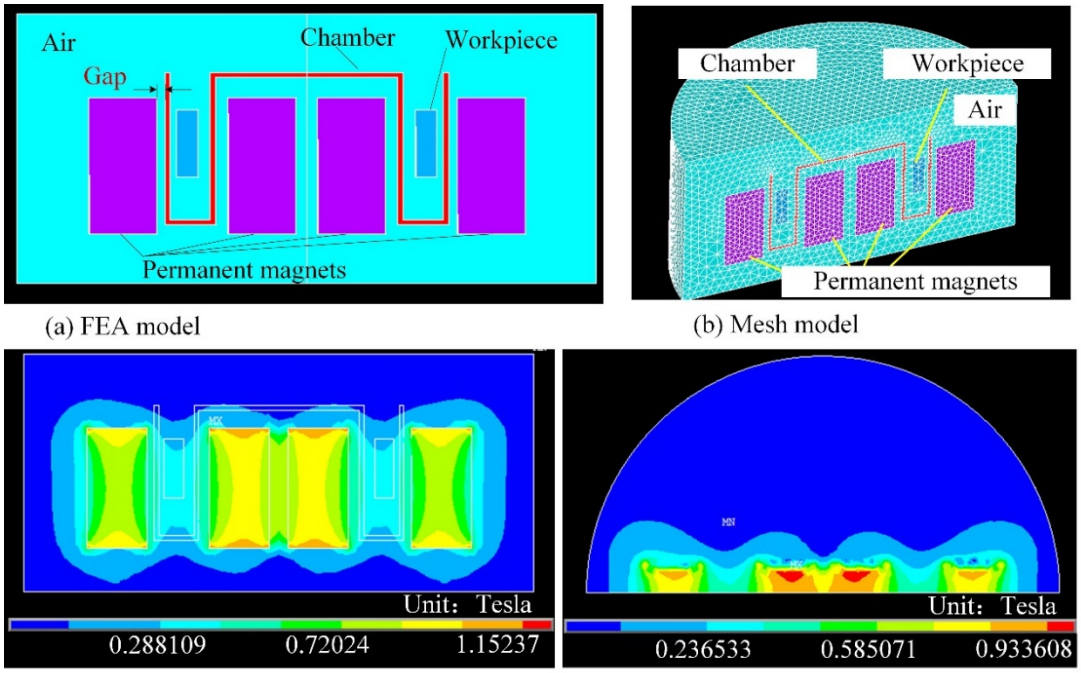

Fig. 2. FEM simulation of the magnetic field distribution

3. Experimental procedures

As shown in Fig. 3, the prototype of the MAMP system was built to evaluate the feasibility of this method. Four N52 Neodymium permanent magnets (size: 25.4 mm×25.4 mm × 50.8 mm, made by CMS Magnetics Inc., USA) were mounted on a rotary table driven by a servo motor. The annular chamber was mounted above the magnets. According to the mechanical design in this study, six workpieces can be polished simultaneously. Moreover, the number of the workpiece can be further increased through changing the design of the fixture. The workpiece material was 304 stainless steel, while the target surface was a cylindrical surface with radius of curvature of 15 mm. The workpiece was mounted with the target surface facing the external wall of the chamber. Fig. 4 shows that two kinds of bonded magnetic abrasives were used in this study. The size of the large bonded magnetic abrasive was about 500~1000 μm, made of iron particles (i.e. 100-200 μm, 80 wt.%) and alumina abrasive (i.e. ~2 μm in average, 20 wt.%). The size of the smaller one is about 200-300 μm, made of iron particle (i.e. ~20 μm, 80 wt.%) and alumina abrasive (i.e. ~2 μm in average, 20 wt.%). Another loose magnetic abrasive is composed of a carbonyl iron particle (CIP) (i.e. ~3 μm in average, 76.7 wt.%), and polishing slurry (i.e. 150 nm alumina mixed with carrier fluid, 23.3 wt.%, hastilite polynano alumina, Universal Photonics Inc.). Other experimental conditions are summarized in Table 1. And three times of repetitions were conducted under each different conditions.

Since this experimental prototype is the first version of the MAMP device, the first priority in this stage is to find out the effect of each key parameters. Hence, single factor analysis was used to design the experiments as shown in Table 1. The surface roughness

of the workpiece was evaluated adopting the arithmetic mean height of the surface (Sa) using a Zygo Nexview optical interferometer. The material removal was evaluated in terms of the workpiece weight difference before and after polishing, measured by an electrical balance with 0.001 gram (1 mg) of resolution. The surface roughness and surface form profile and was measured by a Form Talysurf PGI1240. The surface micro topography of the workpiece before and after polishing was examined by a Hitachi Electron Microscope TM3000.

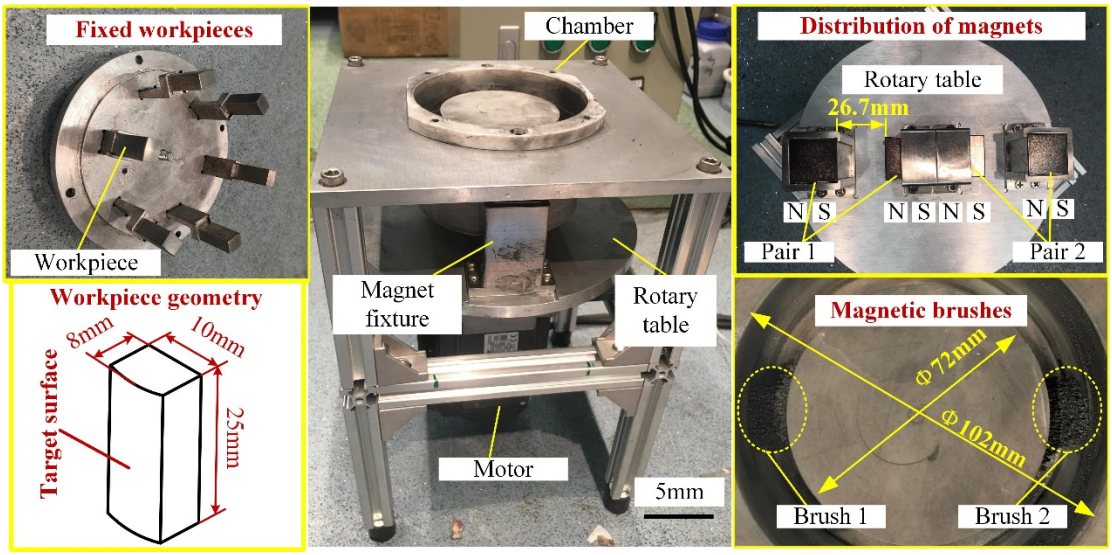

Fig. 3. Prototype of magnetic-field assisted mass polishing system

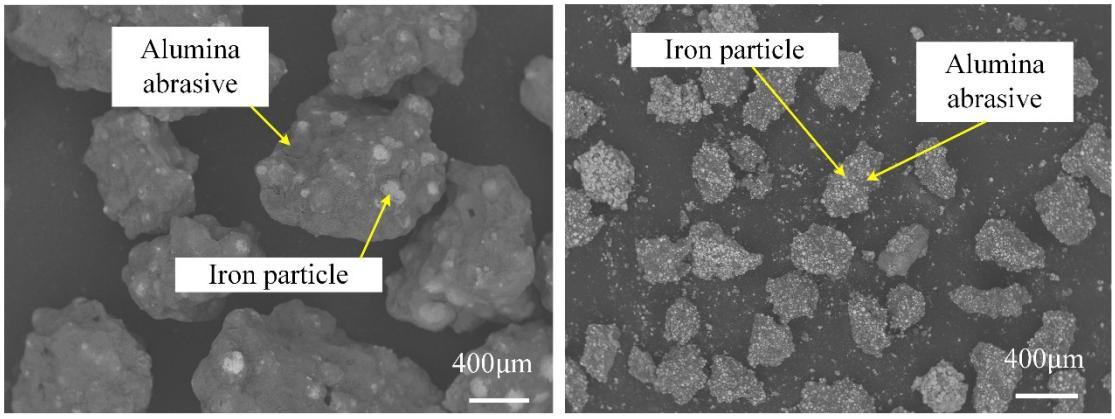

(a) Large bonded magnetic abrasive (b) Small bonded magnetic abrasive

Fig. 4. SEM photograph of the fabricated bonded magnetic abrasives (Measured on Hitachi Electron Microscope TM3000)

Table 1 Experimental conditions

Conditions	Value
Polishing time (min)	5-30
Rotational speed (rpm)	100-2000
Gap between magnet and chamber[a]	1mm, 5mm, 9mm
Weight of bonded magnetic abrasive (g)	50
Lubricant	5 ml silicon oil
Workpiece material	304 stainless steel
Weight of loose magnetic abrasive fluid (g)	110
Surface initial roughness (nm)	200-1200

[a]The gap has been shown in Fig. 2(a).

4. Results and discussion

4.1 performance analysis of the polished surfaces

Fig. 5 shows the cylindrical surface of the workpiece before polishing, and a mirror surface was successfully obtained after rough polishing following by fine polishing. The surface roughness before polishing was 455.4 nm. Large bonded magnetic abrasives were used in rough polishing. The rotational speed of the MAMP system was 1500 rpm, and the gap distance between the magnet and the chamber was 1 mm. After

30 minutes of rough polishing, the surface roughness was decreased to S_a 49.8 nm. The loose magnetic abrasive was used for fine polishing, and S_a 13.8 nm was obtained after 20 minutes of polishing. The convergence rate of the surface roughness reaches 96.97% after the MAMP process, and the surface integrity of the polished surface was quite good as shown in Fig. 5, which indicates the feasibility of this novel process. Moreover, the surface profile before and after polishing were also compared through measuring the center generatrix of the cylindrical surface. Three surface profiles of the initial surface, after rough polishing and fine polishing have all been presented in Fig. 6. Moreover, three of them were also compared as shown in Fig. 6, which indicates good form accuracy of the workpiece can be maintained by the MAMP process when the cylindrical surfaces are polished.

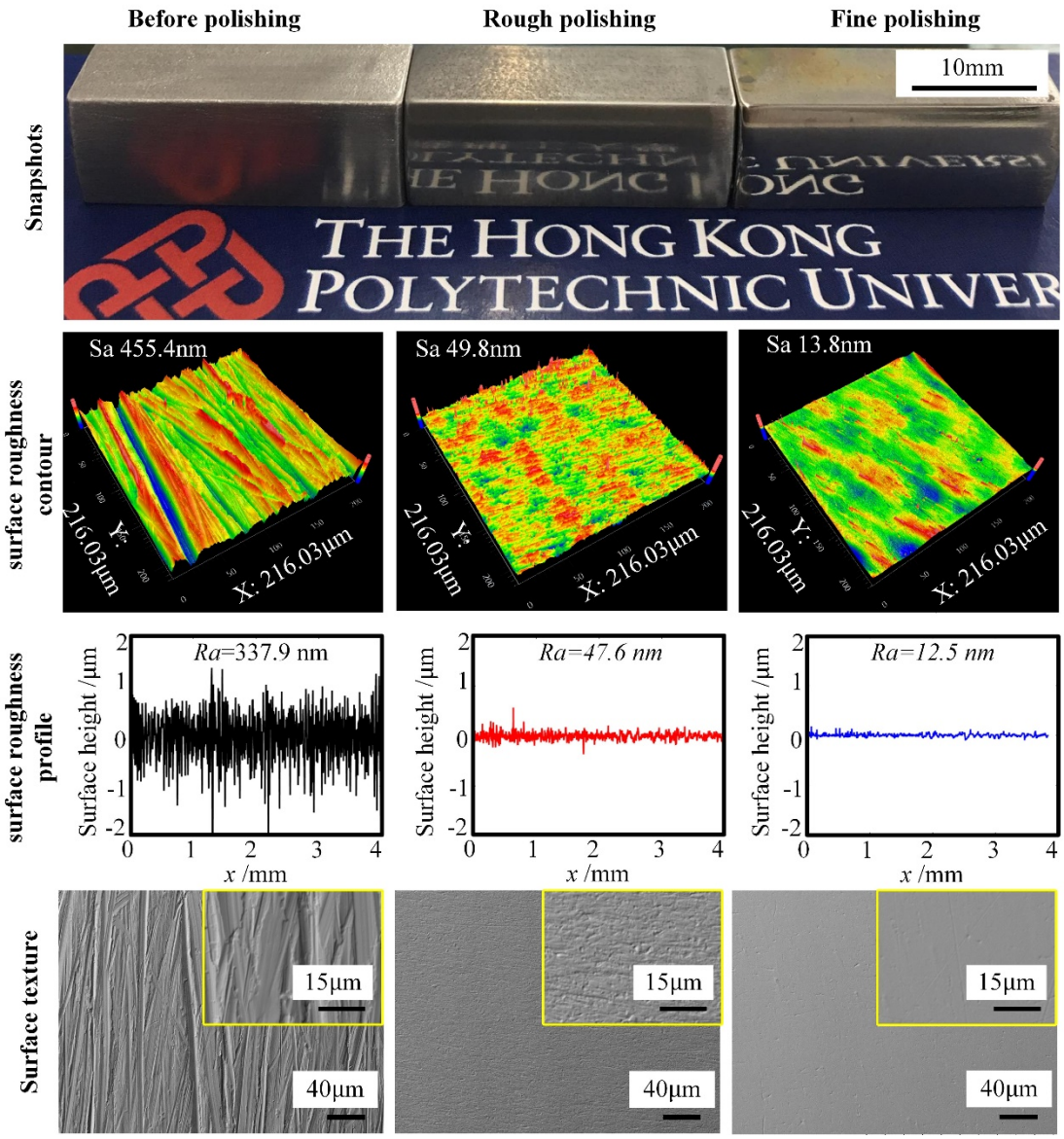

Fig. 5. Surface integrity of the workpiece before and after MAMP

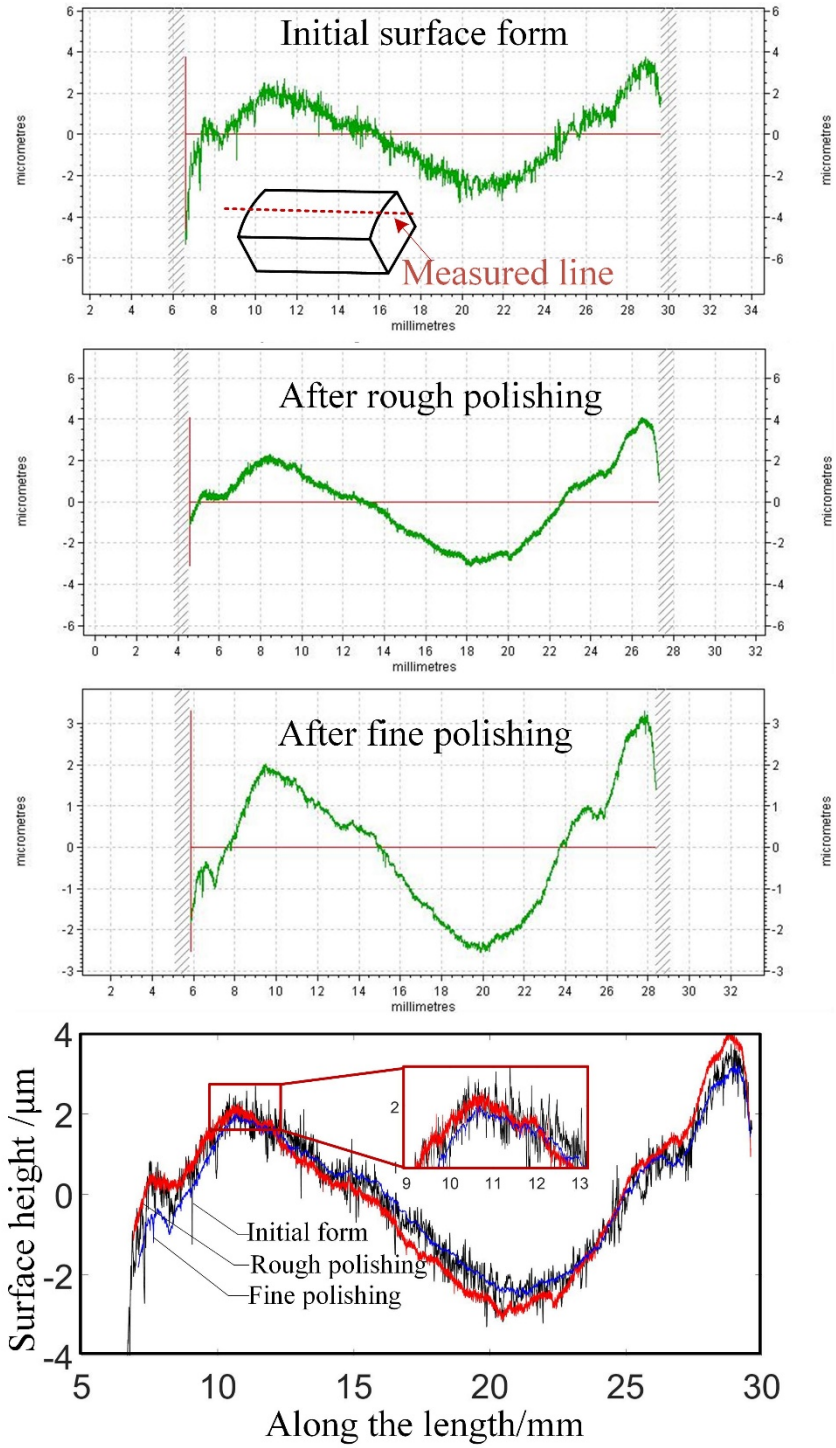

Fig. 6. Analysis of the surface form before and after MAMP

4.2. Effect of the polishing time

Effect of the polishing time to the material removal was studied on three different

workpieces with different initial surface roughness including 1137.1 nm (1# workpiece), 411.8 nm (2# workpiece), and 247.2 nm (3# workpiece). Large bonded magnetic abrasives were used in this group of experiments. The results are shown in Fig. 7.

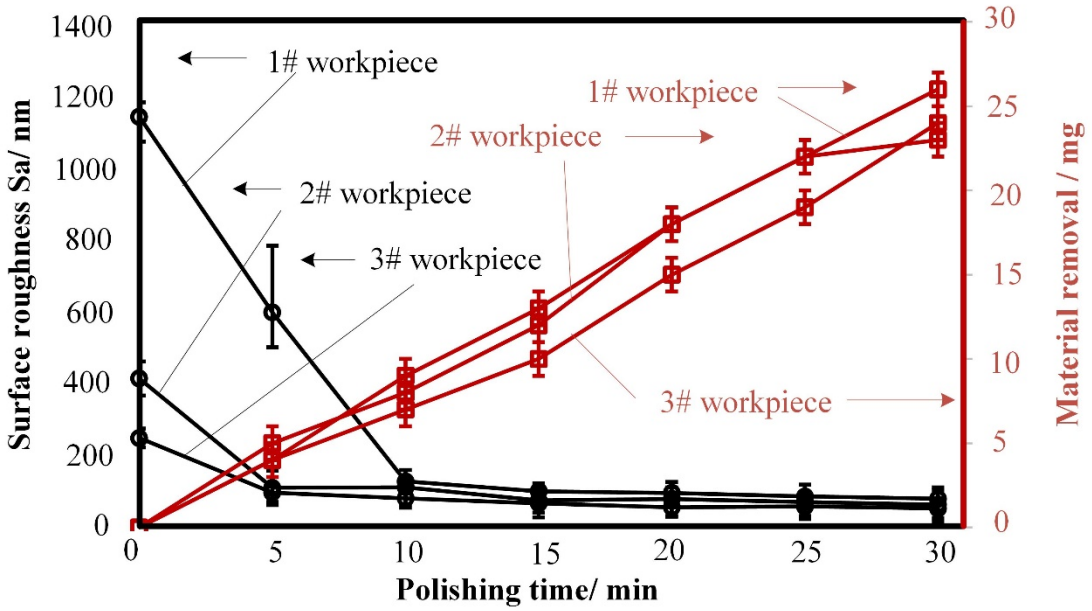

Fig. 7. Material removal and surface roughness changing with the polishing time.

Significant reduction of the surface roughness was found in the first 10 minutes, and almost converged to the lowest surface roughness after 15 minutes of polishing. The surface roughness converged to almost the same value for the three samples, since they were polished using the same magnetic abrasives and under the same polishing conditions. Moreover, the material removal increased basically proportionally to the polishing time irrespective of the workpiece initial surface roughness, indicating that the MAMP process is controllable by the polishing time.

4.3. Effect of magnetic abrasives

Three different kinds of magnetic abrasives were used in this study, including large

and small bonded magnetic abrasives, as well as loose magnetic abrasive. The results of the material removal and surface roughness changing with the polishing time is shown in Fig. 8. It was found that the material removal using large bonded magnetic abrasive was the largest, while that for the loose magnetic abrasive was the smallest and even smaller than the small bonded magnetic abrasive. This is induced by that the magnetic force of the large bonded magnetic abrasive is much larger, depending on the large volume of the magnetic particles according to Eq. (1). With the large material removal, the surface roughness could be reduced within a short period of time comparing to the other kinds of abrasives. Hence, the large bonded magnetic abrasives are suitable to be used for rough polishing to achieve large material removal, while the loose magnetic abrasives are suitable to be used for fine polishing to achieve nanometric surface finish.

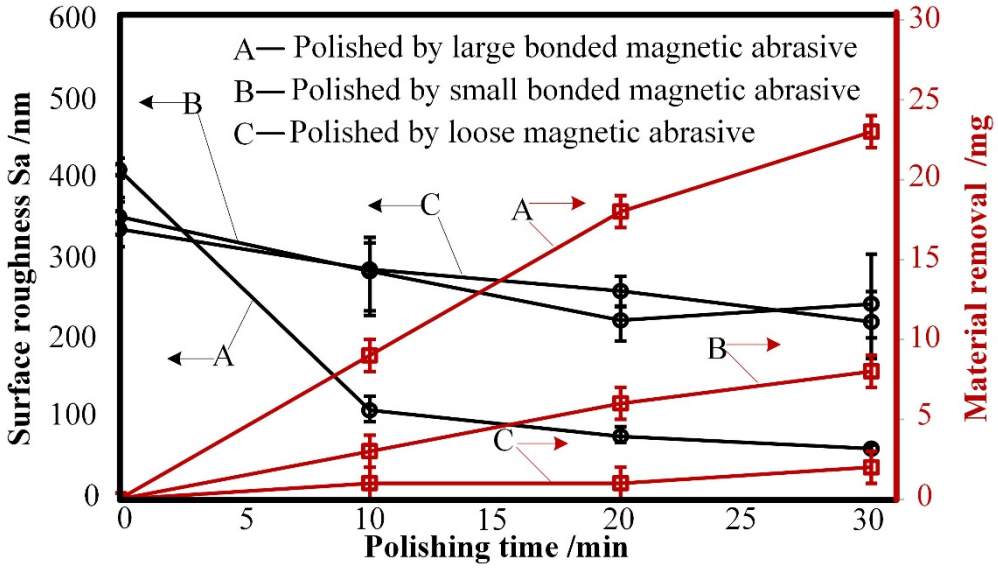

Fig. 8. Material removal and surface roughness changing with the polishing time using different kinds of magnetic abrasives

4.4. Effect of rotational speed of the magnetic brush

The rotational speed of the magnetic brush is controlled by the rotational speed of the rotary table of the MAMP system which is a key process parameter of the MAMP process. In this experiment, five cylindrical surfaces with almost the same initial surface roughness were polished under different rotational speeds. The gap distance between the magnet and the chamber was 1 mm. Fig. 9 shows the results of the effect of rotational speed on material removal and surface roughness.

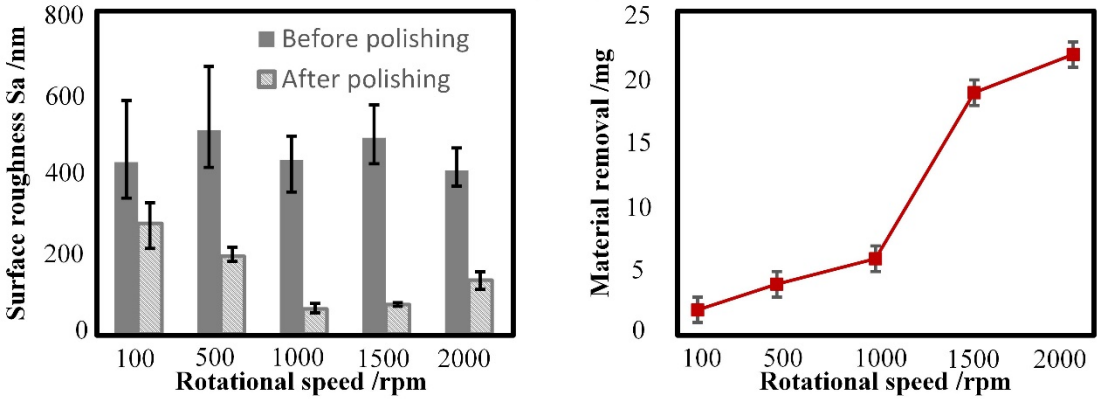

Fig. 9. Material removal and surface roughness varied with the rotational speed.

The surface roughness was found to decrease with increasing rotational speed until the rotational speed of 1500 rpm. However, when the rotational speed was increased to 2000 rpm, the surface roughness increased. The reason is that the centrifugal force increases with the increasing rotational speed, which leads to an increase of the frictional force exerted on each abrasive, and the magnetic force can hardly overcome the frictional force so as to maintain smooth rotation. This leads to the magnetic brush out of synchronization, which results in irregular jumbling of the magnetic abrasives

which are aggressively impinged on the workpiece surface thereby affecting the surface improvement. (Yamaguchi and Shinmura, 2000) The sound generated during polishing varies when the rotational speed is increased to 2000 rpm while being different with that at a lower speed. As a result, higher magnetic force should be exerted to maintain smooth rotation of the magnetic abrasives under a high rotational speed. This phenomenon is similar to that mentioned in the inner surface magnetic abrasive finishing process, as reported by Yamaguchi and Shinmura (2000). It was also found that the increasing rotational speed can cause the increase of the material removal. This is due to the fact that a higher rotational speed leads to a higher impinging velocity of the abrasive, which attributes to a larger material removal. However, the rate of material removal decreased with increasing rotational speed to 2000 rpm, which may be caused by the jumbling phenomenon of the magnetic abrasive.

4.5. Effect of the magnetic flux density

In the MAMP system, the magnetic flux density inside the chamber is controlled by changing the gap distance between the magnet and the chamber wall. Three groups of polishing experiments were conducted under different gap distances so as to analyze the influence of the magnetic flux density on surface generation. The large bonded magnetic abrasive was used and the rotational speed was 1500 rpm. Fig. 10 shows the variation of the material removal and surface roughness. It was found that the material removal decreased with increasing gap distance. The surface roughness decreased in a shorter period of time when the gap distance decreased. The reason is that a decrease

of gap distance increases the magnetic flux density in the chamber. A higher magnetic flux density leads to a larger magnetic force based on Eq. (1) and Eq. (2).

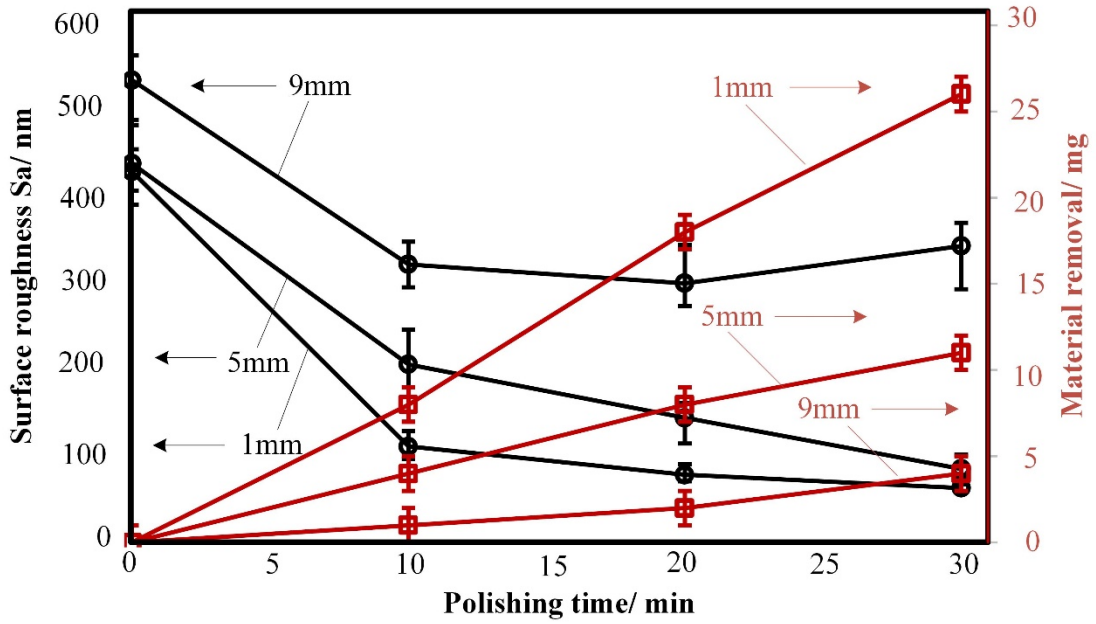

Fig. 10. Material removal and surface roughness changing with different magnetic flux density under various gap distances

To explain the effect of the gap distance on the magnetic flux density, a FEM simulation experiment was conducted under different gap distances. Figure 11 shows the simulation results of the magnetic flux density distribution of three different cases with different gap distances. The measurement of the magnetic flux density was also conducted inside the chamber using a hall sensor with a 1×10^{-5} T resolution. The magnetic flux densities in the centre of the chamber along the radial direction were extracted and compared as shown in Fig. 12. Even though there exists differences between the simulation and measured results induced by the modelling assumptions, etc., the simulated magnetic flux density agrees reasonably well with the measured data in terms of the variation trend. This validates the FEM model. It is noted that the

magnetic flux density inside the chamber increases with reducing gap distance, which explains the relationship between the material removal and the magnetic flux density.

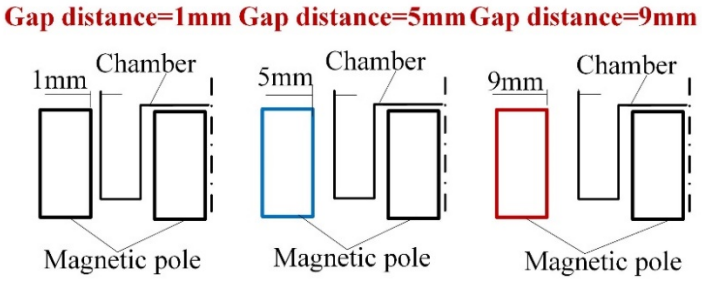

(a) Three cases of different magnetic flux density through changing the gap distance

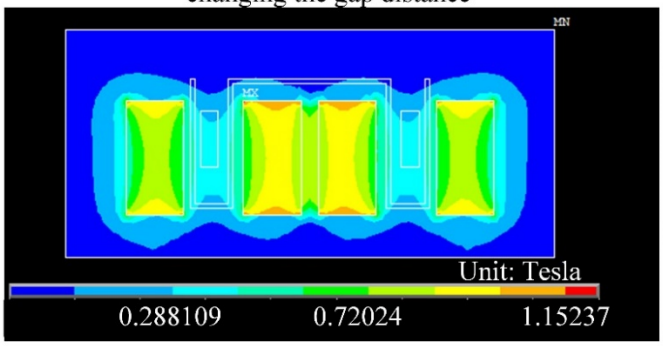

(b) Simulation results of magnetic flux density: gap distance=1mm

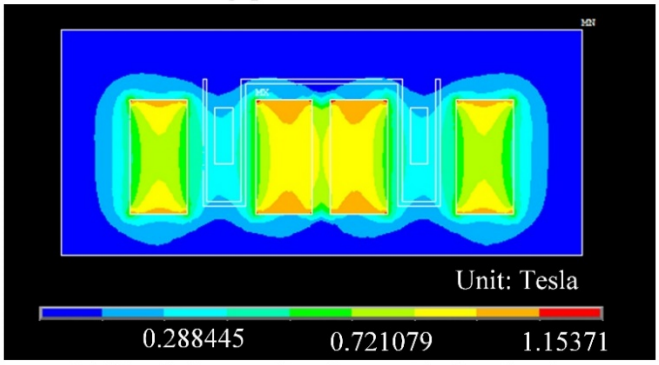

(c) Simulation results of magnetic flux density: gap distance=5mm

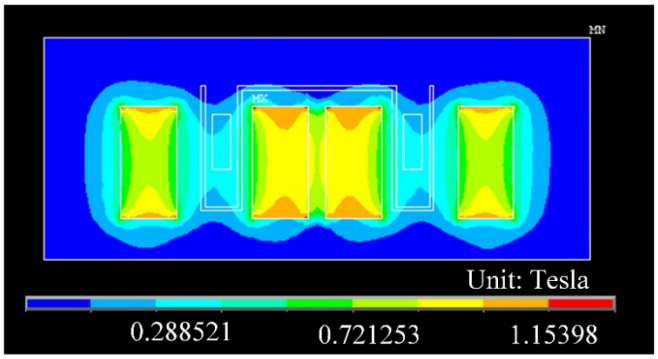

(d) Simulation results of magnetic flux density: gap distance=9mm

Fig. 11. Simulation results of the magnetic flux density distribution with three different gap distances

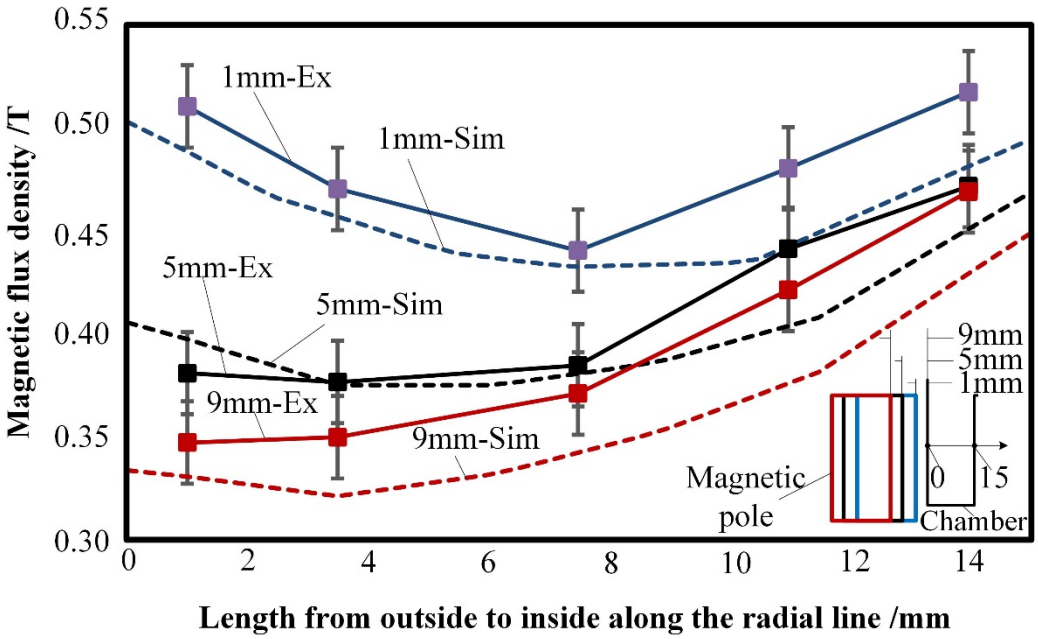

Fig. 12. Magnetic flux density analysis inside the chamber varies with the gap distance. (1mm-Ex signifies the experimental results of 1mm gap distance, 1mm-Sim signifies the simulation results of 1mm gap distance.)

4.6. Application to freeform surface polishing

To demonstrate the applicability of the MAMP method and system for mass polishing of freeform surface components, a series of polishing experiments was conducted on a freeform surface composed of an aspheric surface at the central area and flat surfaces at four corners of the surface (see Fig. 13). This is a mould insert surface of a radar transmitting lens. The surface function of the central aspheric surface has also been shown in Fig. 13. The initial surface roughness of the workpiece was 261 nm. Rough polishing was conducted by using the large bonded magnetic abrasives for 30 minutes

using a rotational speed of 1500 rpm and 1mm gap distance, according to the performance analysis above. Fine polishing was conducted for 20 minutes using the loose magnetic abrasive. The surfaces before and after polishing are shown in Fig. 13. The surface roughness of the workpiece after fine polishing was found to be Sa 15.0 nm. This demonstrates the feasibility of the MAMP process for mass finishing of freeform surfaces with nanometric surface roughness.

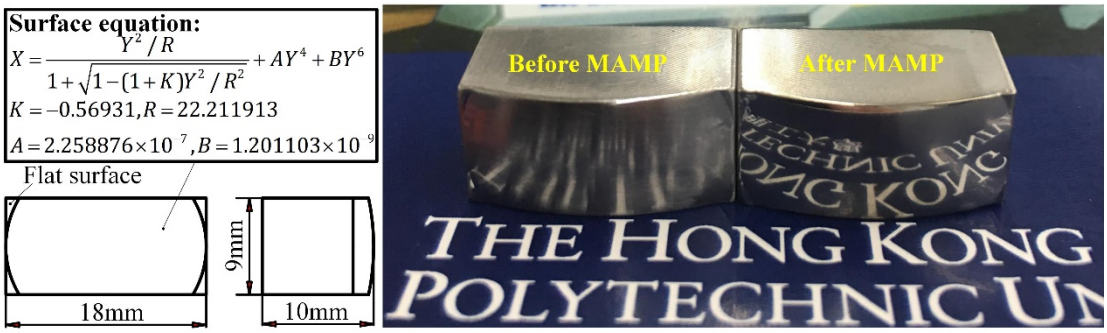

Fig. 13. Freeform surface before and after MAMP.

5. Conclusions

A novel magnetic field-assisted mass polishing (MAMP) method was presented in this paper, and hence a MAMP system which were purposely developed for high-efficiency polishing of a number of freeform components with nanometric surface finish. The feasibility of the MAMP process has been validated through a series of polishing experiments. The effects of the key factors affecting the material removal and surface roughness were also studied. The key factors include polishing time, properties of the magnetic abrasives, gap distance and rotational speed of the magnetic brush. The results demonstrate the technical feasibility and controllability of this novel MAMP process for mass finishing of freeform components with nanometric surface roughness.

And both bonded magnetic abrasive and loose magnetic abrasive could be used in the MAMP process for rough and fine polishing, respectively. Further research will be carried out for the mass polishing of freeform surfaces made of other materials (e.g. optical glass, silicon carbide, etc.) and different magnetic abrasives.

Acknowledgements

The authors would like to express their sincere thanks for the financial support from the Research Office (Project code: BBX7). We also sincerely thanks BASF Germany for providing carbonyl iron powders for our research work.

References

Chang, G.W., Yan, B.H., Hsu, R.T., 2002. Study on cylindrical magnetic abrasive finishing using unbonded magnetic abrasives. International Journal of Machine Tools and Manufacture 42(5), 575-83.

Davidson, D.A., 2007. Green mass finishing with dry abrasive and polishing media: novel finishing process allows refined surface edge effects while avoiding conventional wet-waste discharge. Metal finishing 105(5), 45-48.

Fang, F.Z., Zhang, X.D., Weckenmann, A., Zhang, G.X., Evans, C., 2013. Manufacturing and measurement of freeform optics. CIRP Annals-Manufacturing Technology 62(2), 823-46.

Fang, F., Zhang, N., Guo, D., Ehmann, K., Cheung, B., Liu, K. and Yamamura, K., 2019. Towards atomic and close-to-atomic scale manufacturing. International Journal of Extreme Manufacturing, 1(1), 012001.

Furuya, T., Wu, Y., Nomura, M., Shimada, K. and Yamamoto, K., 2008. Fundamental performance of magnetic compound fluid polishing liquid in contact-free polishing of metal surface. Journal of Materials Processing Technology 201(1-3), 536-541.

Guo, J., Tan, Z.E., Au, K.H. and Liu, K., 2017. Experimental investigation into the effect of abrasive and force conditions in magnetic field-assisted finishing. The International Journal of Advanced Manufacturing Technology 90(5-8), 1881-1888.

Guo, J., Au, K.H., Sun, C.N., Goh, M.H., Kum, C.W., Liu, K., Wei, J., Suzuki, H. and Kang, R., 2019. Novel rotating-vibrating magnetic abrasive polishing method for double-layered internal surface finishing. Journal of Materials Processing Technology 264, 422-437.

Hashimoto, F. and DeBra, D.B., 1996. Modelling and optimization of vibratory finishing process. CIRP annals, 45(1), 303-306.

Hashimoto, F., and Johnson, S.P., 2015. Modeling of vibratory finishing machines. CIRP Annals-Manufacturing Technology 64(1), 345-348.

Hashimoto, F., Yamaguchi, H., Krajnik, P., Wegener, K., Chaudhari, R., Hoffmeister, H.W., and Kuster, F., 2016. Abrasive fine-finishing technology. CIRP Annals-Manufacturing Technology 65(2), 597-620.

Jain, V.K., 2009. Magnetic field assisted abrasive based micro-/nano-finishing. Journal of Materials Processing Technology 209(20), 6022-6038.

Jha, S., Jain, V.K., 2004. Design and development of the magnetorheological abrasive flow finishing (MRAFF) process. International Journal of Machine Tools and Manufacture 44(10), 1019-1029.

Komanduri, R., Lucca, D.A., Tani, Y., 1997. Technological advances in fine abrasive processes. Annals of CIRP 46 (2), 545–596.

Kordonski, W. I., & Jacobs, S. D., 1996. Magnetorheological finishing. International Journal of modern physics B 10(23-24), 2837-2848.

Kumar, S., Jain, V.K. and Sidpara, A., 2015. Nanofinishing of freeform surfaces (knee joint implant) by rotational-magnetorheological abrasive flow finishing (R-MRAFF) process. Precision engineering 42, 165-178.

Li, W., Li, X., Yang, S. and Li, W., 2018. A newly developed media for magnetic abrasive finishing process: Material removal behavior and finishing performance. Journal of Materials Processing Technology 260, 20-29.

Li, X., Li, W., Yang, S., Hao, Z. and Shi, H., 2018. Study on polyurethane media for mass finishing process: Dynamic characteristics and performance. International Journal of Mechanical Sciences 138, 250-261.

Shinmura, T., Takazawa, K., Hatano, E., Matsunaga, M., and Matsuo, T., 1990. Study on magnetic abrasive finishing. CIRP Annals-Manufacturing Technology 39(1), 325-328.

Singh, A.K., Jha, S. and Pandey, P.M., 2011. Design and development of nanofinishing process for 3D surfaces using ball end MR finishing tool. International Journal of Machine Tools and Manufacture 51(2), 142-151.

Uhlmann, E. and Eulitz, A., 2018. Wear Mechanisms of Ceramic Vibratory Finishing Media. Nanomanufacturing and Metrology 1(2), 96-104.

Yamaguchi, H., and Shinmura, T., 2000. Study of an internal magnetic abrasive

finishing using a pole rotation system: Discussion of the characteristic abrasive behavior. Precision Engineering 24(3), 237-244.

Yamaguchi, H., Kang, J., Hashimoto, F., 2011. Metastable austenitic stainless steel tool for magnetic abrasive finishing. CIRP Annals-Manufacturing Technology 60(1), 339-42.

Yamaguchi, H. and Graziano, A.A., 2014. Surface finishing of cobalt chromium alloy femoral knee components. CIRP Annals-Manufacturing Technology 63(1), 309-312.

Yamaguchi, H., Nteziyaremye, V., Stein, M., and Li, W., 2015. Hybrid tool with both fixed-abrasive and loose-abrasive phases. CIRP Annals-Manufacturing Technology 64(1), 337-340.

Zhang, Z., Yan, J. and Kuriyagawa, T., 2019. Manufacturing technologies toward extreme precision. International Journal of Extreme Manufacturing 1, 022001.